Workshop: MR Imaging of X-Nuclei (^{23}Na & Friends): From Controversies to Potential Clinical Applications

Title of talk: Multiple quantum effects in X nuclei MRI

Gil Navon, navon@post.tau.ac.il

School of Chemistry, Tel Aviv University, Tel Aviv, Israel

Highlights

- Theory of multiple quantum filtered NMR and MRI
- Examples in the fields of musculoskeletal and nervous systems

1. Introduction

Dipolar and quadrupolar interactions tend to average out in molecules that undergo fast isotropic tumbling motions, giving rise to high resolution spectra. However in cases of slow and/or anisotropic motion the residual dipolar and quadrupolar interactions are manifested as line broadening and splittings. In multiple quantum filtered NMR, the sharp signals resulting from complete averaging of the dipolar and quadrupolar interactions are filtered out and thus accentuate the effects of molecules that are bound to macromolecules or that reside in ordered environments. This is particular valuable in biological systems where ordered systems such as fibers and membranes impose anisotropic motion on water molecules and sodium ions. As a result, the ^{1}H dipolar and ^{2}H and ^{23}Na quadrupolar interactions do not average to zero but manifest values that are scaled down from their solid-state values. As a consequence, the NMR lineshapes either exhibit clear splittings in the case of macroscopic order, or inhomogeneous broadening in the case of random distribution of motion directors. The manifestation of a residual proton-proton dipolar interaction in water molecules is hampered by the proton exchange reaction between water molecules[1]. This exchange occurs at a rate of about 3500 s^{-1} at room temperature[2,3]. Thus only systems with water residual ^{1}H-^{1}H dipolar interactions greater than this value will exhibit resolved splittings, while lower values of this interaction will result in line broadening. This difficulty is alleviated when measurements are performed using ^{2}H since the dominant interaction of this nucleus is quadrupolar and not affected by the exchange of the deuterium atoms between water molecules. Thus, studies of D_2O in tissues can be more informative from a magnetic resonance standpoint, than those of H_2O. ^{23}Na is the second most abundant NMR-active nucleus in biological tissues, after ^{1}H. In addition to its central role in many physiological processes, this makes it an attractive nucleus for biomedical NMR and MRI research[4-6].

2. Theoretical Background

The basic multiple quantum filtered (MQF) pulse sequence is given by:

$90^o - \tau/2 - 180^o - \tau/2 - \theta^o - t_{MQ} - \theta^o$ (acq) . [1]

A convenient way to describe the various processes occurring during the pulse sequence is by the irreducible spherical tensor operator basis, $T_{l,p}$. Here l is the rank and p is the coherence of the tensor

with $|p| \leq l$. These tensors are composed of combinations of the more familiar spin operators Iz and $I_{\pm} = Ix \pm iIy$. For example, some of the relationships that apply for spin $I \geq 1$ nuclei are given in the table:

Spherical tensors	Single $I \geq 1$ spin
$T_{1,0}$	I_{1z}
$T_{1,\pm1}$	$\mp\frac{1}{\sqrt{2}}I_{\pm}$
$T_{2,0}$	$\frac{1}{\sqrt{6}}(3I_z^2 - I^2)$
$T_{2,\pm1}$	$\mp\frac{1}{2}(I_zI_{\pm} + I_{\pm}I_z)$
$T_{2,\pm2}$	$\frac{1}{2}I_{\pm}^2$

This representation has the advantage of facilitating the understanding of the processes occurring during the pulse sequences. Following the sequence of events requires bearing in mind the two simple rules that apply at high magnetic fields: (a) a non-selective radiofrequency pulse can change the coherence order p within the limits of $|p| \leq l$; and (b) changes in the rank l can occur by relaxation and modulation by quadrupolar interaction (as well as by dipolar and J-coupling for a couple of spin 1/2 nuclei), while keeping the value of p unchanged. The coherence pathway of the MQF pulse sequence (Eq.1) is given in Fig. 1[7]. Double quantum (DQ) and triple quantum (TQ) coherences are detected separately by proper phase cycling.[8]

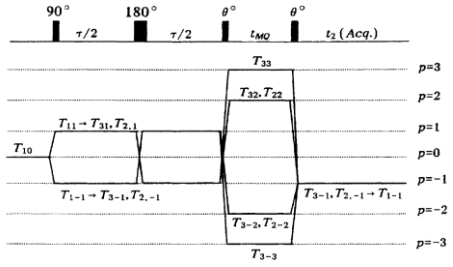

For spin I=3/2 nuclei the SQ transverse relaxation is biexponential, characterized by two relaxation times T_{2f} and T_{2s}. In cases where the residual quadrupolar interaction (ω_Q) is greater than the fast T_2 relaxation rate $\omega_Q >> 1/T_{2f}$, the double quantum filtered signal is given by[9-11]:

$$\text{Signal}^{DQF} \propto \sin(\omega_Q\tau)e^{-\tau/T_{2f}} - \frac{1}{4}(3\cos^2\theta - 1)^2 \left\{e^{-\tau/T_{2s}} - \cos(\omega_Q\tau)e^{-\tau/T_{2f}}\right\} \qquad [2]$$

When θ is selected to be 54.7° ("magic angle", MA), only second-rank tensors are formed and therefore in the case of ^{23}Na (I=3/2) only sodium experiencing anisotropic motion is detected. In that case, the sequence is called DQF-MA.

The signal after triple quantum filteration is given by:

$$\text{Signal}^{TQF} \propto \left\{e^{-\tau/T_{2s}} - \cos(\omega_Q\tau)e^{-\tau/T_{2f}}\right\} \qquad [3]$$

Here the observed magnetization is composed of a single term which originates from $T_{3,1}$, since second rank tensors cannot give rise to triple quantum coherences.

For spin I=1 third-rank tensors cannot be created and in this case Eq.1 is used with θ=90° for maximum intensity and the signal is given by:

$$\text{Signal}^{DQF} \propto \text{Sin}(\omega_Q\tau)e^{-\tau/T_2} \qquad [4]$$

An in-phase version of the DQF pulse sequence is given by[12]:

90^o - τ - 90^o - t_{DQ} -90^o - τ - 90^o - t_{LM} - 90^o (acq) [5]

This sequence is denoted as DQF-MT since during the longitudinal magnetization time t_{LM} magnetization transfer may occur. In that case the signal is proportional to:

$$\text{Signal}^{\text{DQF-MT}} \propto \text{Sin}^2(\omega_Q \tau) e^{-2\tau/T_2} . e^{-t_{LM}[(1/T_1)+k_{MT}]} \qquad [6]$$

3. Example #1: ^{2}H DQF studies of the effects of mechanical load and osmotic pressure on the collagen network in articular cartilage.[13,14]

The importance of articular cartilage in the development of osteoarthritis and the remarkable viscoelastic properties of this tissue has generated an extensive amount of research devoted to the study of cartilage under load. However, most of the studies are very invasive, involved detaching the cartilage from the bone, and fixation. When pressure is applied to cartilage, water is forced out of the extracellular matrix, the concentration of the PG increases, resulting in an increase of the swelling pressure. Due to the technical difficulties in performing the measurements under mechanical pressure, osmotic stress has been used as a model for the in vivo loaded tissue since the same levels of dehydration can be achieved by applying the osmotically active solutions of polyethyleneglycol (PEG) and an equivalent mechanical load. The splitting of the ^{2}H spectra on cartilage equilibrated in deuterated saline is related to the density and the degree of order of the collagen fibers. Fig 2 shows spectroscopic MRI of bovine articular cartilage-bone plug equilibrated in deuterated saline under stepwise application of mechanical pressure. At the end of the experiment, the plug was re-equilibrated and measured again.

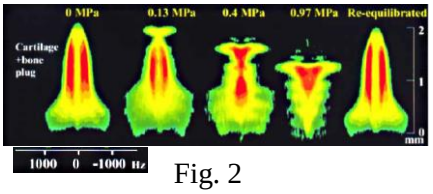

Fig. 2

As expected from the known structure of cartilage without load, the well-ordered collagen fibers perpendicular to the bone surface near the bone give large splitting that diminishes toward the surface where the orientation become flat going through the magic angle. The changes in the magnitude of the quadrupolar splitting upon increasing pressure shown in Fig 2 indicate the disruption of the order in the calcified zone. The increased splitting at the surface is caused by buildup of order and as a result of preferential loss of water from the surface zone.

3. Example #2: ^{2}H DQF-MT and ^{23}Na TQF-MT studies of the compartments in nerves and spinal cord

Maximum DQF-MT and TQF-MT signals are obtained for $\omega_Q\tau=\pi/2$ and $\omega_Q\tau=\pi$ respectively. Thus, by changing the creation time τ in MQF pulse sequences it is possible to select the tissue compartments according to their degree of order as expressed in the value of the residual quadrupolar interaction ω_Q. Examples are shown in Figs. 3 and 4 for ^{2}H DQF-MT of rat sciatic nerve and ^{23}Na TQF-MT of bovine optic nerve. Similar spectra are obtained also for spinal cord.

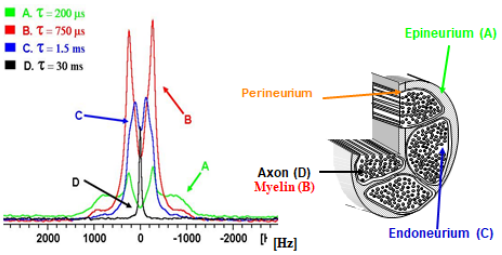

Fig. 3: ^{2}H DQF-MT of rat sciatic nerve

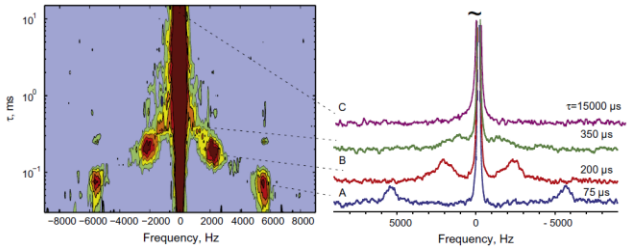

Fig. 4: ^{23}Na TQF-MT of bovine optic nerve

Once the selection is done, it is possible to measure the relaxation times and diffusion properties of each compartment separately. For instance, the narrow peaks in Figs. 3 and 4 exhibit anisotropic diffusion, which is highly restrictive in the perpendicular direction, indicating intraaxonal compartment. During t_{LM} in Eq. 5 chemical exchange between the compartments takes place. Thus, variation of the t_{LM} allows the measurement of the rate constant of this exchange.

References

1. U. Eliav, G. Navon, *J. Magn. Reson.* 1999; **137**: 295.
2. S. Meiboom, *J. Chem. Phys.* 1961; **34:** 375.
3. D. L. Turner, *Mol. Phys.* 1980; **40:** 949.
4. G. Madelin, J. S. Lee, R. R. Regatte, A. Jerschow, *Prog.NMR Spect.* 2014; **79**: 14.
5. P. A. Bottomley, *eMagRes*., 2012; **1**: 353.
6. U. Eliav, G. Navon, *NMR Biomed*., 2016; **29**: 144.
7. G. Navon, H. Shinar, U. Eliav, Y. Seo, *NMR Biomed*., 2001; **14**: 112.
8. G. Bodenhausen, H. Kogler, R. R. Ernst, *J Magn Reson*, 1984; **58**: 370.
9. G. Jaccard, S. Wimperis, G. Bodenhausen, *J. Chem. Phys.* 1986; **85**: 6282.
10. U. Eliav, H. Shinar, G. Navon, *J. Magn. Reson.* 1992; **98**: 223.
11. U. Eliav, G, Navon, *J. Mag. Reson. B*, 1994; **103**: 19.
12. U. Eliav, G, Navon, *J. Mag. Reson.* 1999; **137**: 295.
13. K. Keinan-Adamsky H. Shinar, G. Navon, J. Ortho. Res. 2005; **23:** 109.
14. G. Saar, H. Shinar, G. Navon, Eur. Biophys. J. 2007; **36**: 529.
15. H. Shinar, Y. Seo, G. Navon, J. Magn. Reson. 1997; **129**: 98.
16. Y. Seo, H. Shinar, G. Navon, Magn. Reson. Med.1999; **42**: 461.
17. U. Eliav, X. Xu, A. Jerschow, G. Navon, J. Magn. Reson. 2013; **231**: 61.